European Journal of Molecular & Clinical Medicine
ISSN 2515-8260 Volume 07, Issue 9, 2020

CFD technique based Spectrum Sensor for Hardware-Efficient and Fast Sensing of Cognitive Radio Network

[1]E.Gnana Manoharan, [2]K.Vadivelu,
[1]Assistant Professor/ECE.FEAT., Annamalai University,Tamilnadu,India
gnanamanohar@gmail.com

[2]PhD scholar
ECE Department,Annamalai University,Tamilnadu,India
Email Id: vadivelecepan@gmail.com

Abstract—Cognitive radio (CR) is an innovative technology with profound potential for reducing the spectrum shortage within wireless networks of the next decade. Unlicensed users are able in this technology to reach unused parts of the spectrum, commonly known as white spaces, which increase their use of the spectrum. Each of the unauthorised user nodes needs a spectrum sensor to detect white space to transmit and receive data. In this paper, a Cyclostationary Spectrum Sensor (CFD), for CR skill is available that uses less hardware and less time to sens. The obstacle of designing innovative CFD spectrum sensing algorithms based on frequencies was addressed. In particular, a multi-level resource has been provided for optimization with the VLSI 2048-point FFT module. In regards, outcomes of projected spectrum sensor production analyses are provided for 1024, 2048 and 40.096 FFT size and shape where appropriate detection-probability of 0.9 is offered in the proposed design at -5 dB SNR. It was implanted by FPGA and demonstrates that the hardware usage was improved due to a 100% lowered memory necessity, and that a shortened sensing period of 0.3 ms was indexed.

Keywords- Fourier transform (FFT), fast very-large scale-integration (VLSI), Cognitive radio, field programmable gate-array (FPGA) and spectrum sensing procedure.

1. INTRODUCTION

CR skill reduces the issue of bandwidth shortages by exploiting idle spectrum where the licence users are mentioned to as main users[1]. The spectrum occupancy by PUs (primary User) are tested by cognitive-radio function dependent secondary users (SUs) and accessed opportunistically by such an underutilised spectrum. SU interferences must be alleviated in PU contact and this is possible through the use of the reliable spectrum sensing algorithm that is a primary facilitator of cognitive radiation knowledge [2]. The wasteful use of fixed bandwidth, which indicates that less utilisation of licenced spectrum, is largely responsible for spectrum insufficiency [3]. The earliest distribution of the useful radio spectrum renders it impossible to locate empty frequency ranges. There is also trouble with the concept of delivering modern programmes. The secondary consumer (SU) is entitled to use the approved band without interruption in the non-appearance of the PU. This leads to maximising the usage of spectrum [4]. Critical and especially for the CR scenario is the problem of coexistence with current PU connectivity ties. There is not a symmetrical need for coexistence here since CRs are forbidden to interact with PUs. The development of a contact platform for CRs to share the positions of their existing transmitting bands is also an obstacle. Several spectrum sensing procedures such as matching filter-based sensing need perfect PU detection information. Likewise, the energy-

based spectrum sensing algorithm needs no PU expertise; but it provides lower-to-noise (SNR) areas with degraded detection [5]. Then, also in negative SNR area (very poor SNR), CFD-based Spectrum Sensing would be stronger than matched filters and algorithms based on energy detection, as long as CFD sensing has some know-how regarding SNR[6]. It can be used in the frequency fields; it functions well for higher frequency reliability but has greater computing complexity [7]. The CFD algorithm is more complicated. In this effort, we suggest the design of such a spectrum sensor in the frequency domain so as for the extremely weak channel conditions to achieve accurate detection in lower systems. The biggest task is to reduce the usage of hardware while ensuring ample performance [8]. In these cognitive radio systems (such as IEEE 802.22), the Tf for SU communications frame configuration has a slot to sensor, a sensing time (S) and a $Tf - \check{S}$ length data transfer slot. Therefore in order to sustain potential data speeds, shorter detection time is highly desirable in totalling to the hardware-efficient design of the Spectrum Sensor [9].

We provide architectures for the CFD-based frequency domain for both internal and general blocks. In addition, the resource-shared VLSI architecture for lower hardware usage consists of a 2048point FFT module. In addition, the proposed spectrum sensing algorithm is performed in a detailed performance study for various FFT dimensions. Our architecture is essentially hardware-based in an FPGA platform where it is tested in a real-world manner and contrasted with state-of-the-art implementations.

2. PROPOSED VLSI ARCHITECTURES

The CFD dependent spectrum sensor is seen in the diagram. Suggested spectrum sensor and internal sub-module in fig. 1.

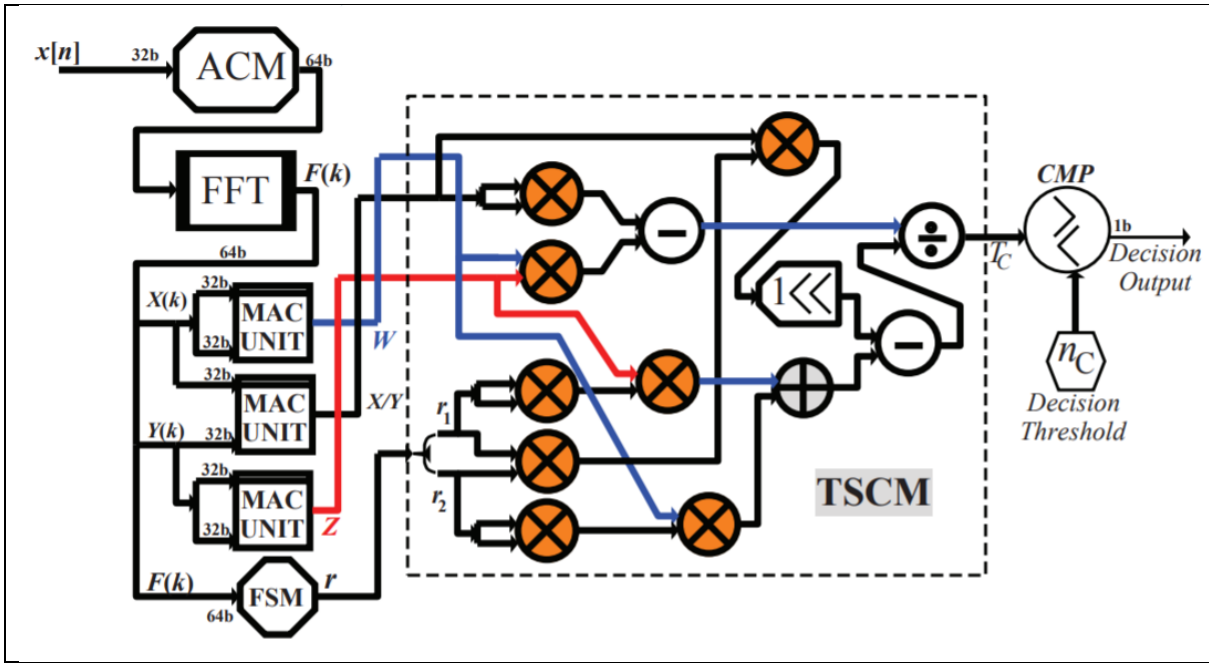

Fig. 1. Architecture of test-statistic computation-module (TSCM)

It indicates that the $x(n)$ of 32-bit input signal is initially processed with the autocorrelation computation module (ACM) (1). It contains the first-input FIFO, a complex conjugate module (CCM) and a 16-bit dynamic multiplier is shown in fig. 2

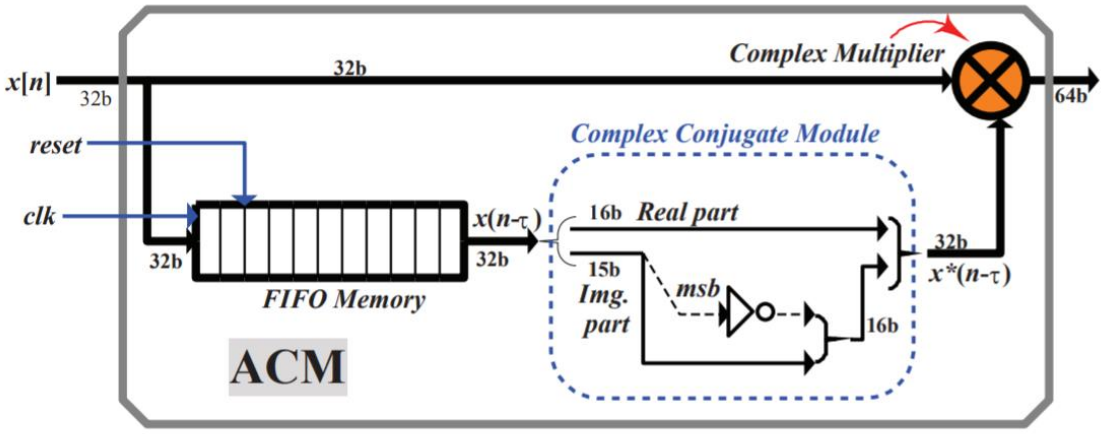

Fig. 2. Autocorrelation computation module (ACM)

The delayed $x(n - \mu)$ version of $x(n)$ and compound conjugated $x(n - ¨)$ is produced here by FIFO register. This value is also complex to produce the value $x(n) \bullet x$ corresponding to that of $x(n - \mu)$ This value is multiplied by $x(n)$. ACM output is fed to the FFT module and Fourier is calculated (k). In particular, the FFT module performs N=22048 (2048 digitised $x(n)$ samples for our spectral sensor). Radix-2 butterfly structure computations. Calculation. The Radix-2 structure consists of 11 stages, and each phase includes three key units: butterfly, double factors and truncation units. In addition, input and output memory blocks to buffer the input as well as calculated FFT values are included in this FFT module. The architecture of the MAC unit has been built using 64-bit, 32-bit multiplier and accumulator displayed in fig. 3.

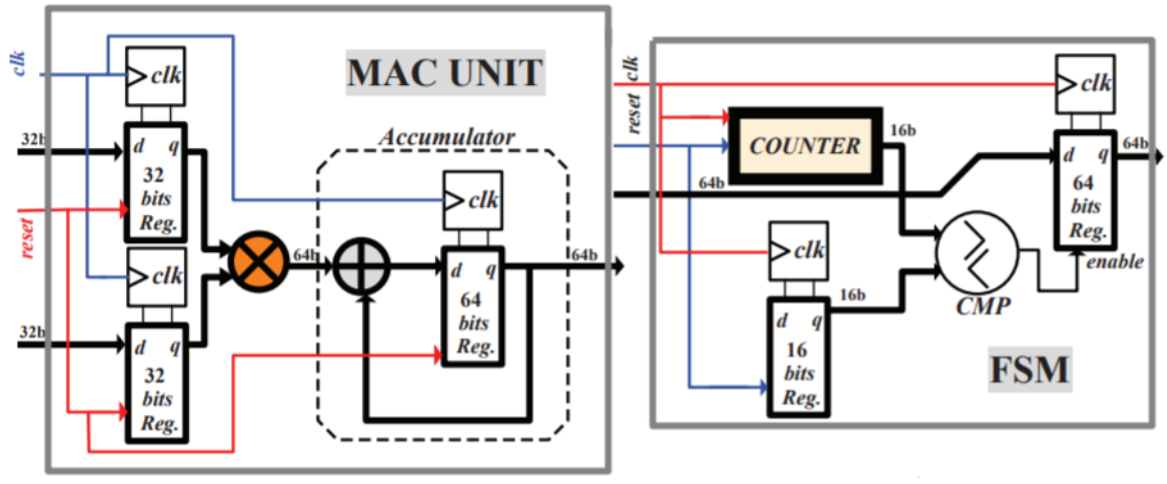

Fig. 3. Multiply-&-accumulate (MAC) unit and FSM

The Frequency Selection Module (FSM), which is located parallel to the MAC modules, is another critical module in our architecture. The performance of FFT module FSM taps F(k) for computing $F(\alpha) = Ré(\alpha, \alpha) = (r1, r2)\ where\ r1 = \{Ré\}\ and\ r2 = \{Ré\}$. Such FSM design requires a 16-bit counter to monitor the contrast iteratively, before the appropriate input

to the output port occurs. Test statistics (Tc), which are measured using a Test Statistical Estimation Module (TCM), are the most significant value for the spectrum sensor, which sum up eight multipliers, two subtractors, one adder, left shifter and divider. This TSCM is compiled with $W, X/Y, Z\ and\ r$ respectively from 3 MAC units and one FSM.

3. PROPOSED FFT-MODULE ARCHITECTURE

The FFT calculation include 11 steps and each of them contains 1024 butterfly frameworks, traditional radix-2 (N=2048 points) algorithm. Due to the direct conversion of such an algorithm to VLSI design, hardware and energy usage would be improved. Therefore, during the development of our FFT spectrum sensor, we propose two levels of hardware mutual services. At the first step, a single process of the FFT unit was commonly circulated, which replaces the necessity of 11 phases, thereby reducing the utilisation of hardware. Secondly, this one-stop sharing of resources of just 64 butterfly structures i.e. Butterfly Measurement I = 1.2, 3 ...64) and LookUp Table (LUTs) containing pre-computed factors of twiddle is substituted by 1024 butterfly structures. This module was named the BCU in our report. This module was included in this post. Here is a single butterfly computer's internal architecture built to provide 64-bit registers, a radix-2 butterfly layout, a dynamic multipliers, a multiplexer for 11:1 and 16:1.

These 64-bit registers stock the input, and multiplexers monitor the drift of twiddle factors controlled by LUTs to our complex architecture multiplier. In this shared resource architecture, the key difficulty lies in translating the right twiddle variables into butterfly constructs by measuring the values for 11 separate phases in the same general resource level. We tackled this problem by producing sufficient tracking signals from the finite-satellite control device (4-bit pick lines with 11:1 and 16:1 multiplexers). Finally, the planned total resource VLSI architecture of projected spectrum sensor is presented in Fig. 4.

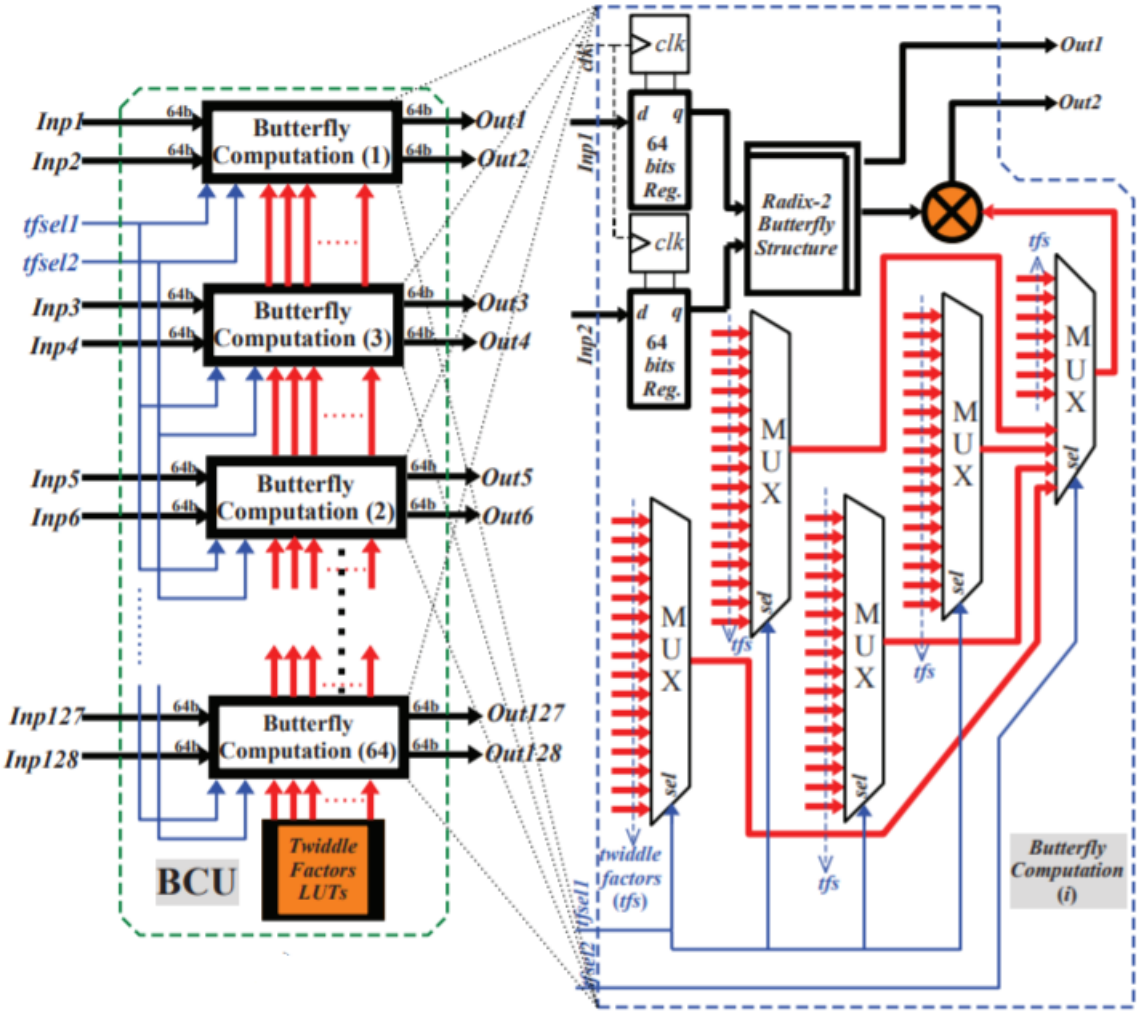

Fig. 4. Projected VLSI-architectures of butterfly computation-unit with butterfly calculation N = 2048 points FFT-module.

The serial-to-parallel registries have been used to provide 64-bit feedback (these include mixture of S/P Converter, 2048 S/P Multiplexer 2048 and INP-REG, which accumulates 2048 64-bit samples each and feeds the BCUs through a 128-clock network, each of which is a 16:1 multiplexer).

4. PERFORMANCE ANALYSIS, FPGA IMPLEMENTATION

The projected frequency domain established spectrum sensor detector efficiency is very sensitive to FFT calculations. The scale of FFT affects the accuracy of which the signal is sent from time to frequency. Table I displays the hardware resource usage and time contrast of our FPGA deployment designs with advanced digital designs for spectrum sensors focused on feature detection. In contrast to current execution, the architecture suggested absorbs a 100% lower (memoryless) memory and a 12.5 times shorter sensing time. In contrast with these findings however, our architecture has considerably higher logic and registration criteria.

Table I hardware source and sensing time

	Parameter metrics

Logic	415048
Memory	0
Register	596783
Sensing time	0.3ms

In this effort, we conducted the proposed spectrum sensor review on 3 separate FFT sizes: 1024, 2048 and 4096. The simulation was conducted via OFDM signals which are produced by the white and gloussian additive noise (AWGN) channel environment under SNR from -26 dB to 0 dB. The simulation is performed here. Each sample is analysed for €1000 to each SNR during this comprehensive simulation. Therefore the identification likelihood against SNR was seen in Figure for various sizes of FFT. 5. The blue figure indicates the FFT 10.24, the red, the FFT 2048, and the black, the FFT 4096, is depicted in this figure.

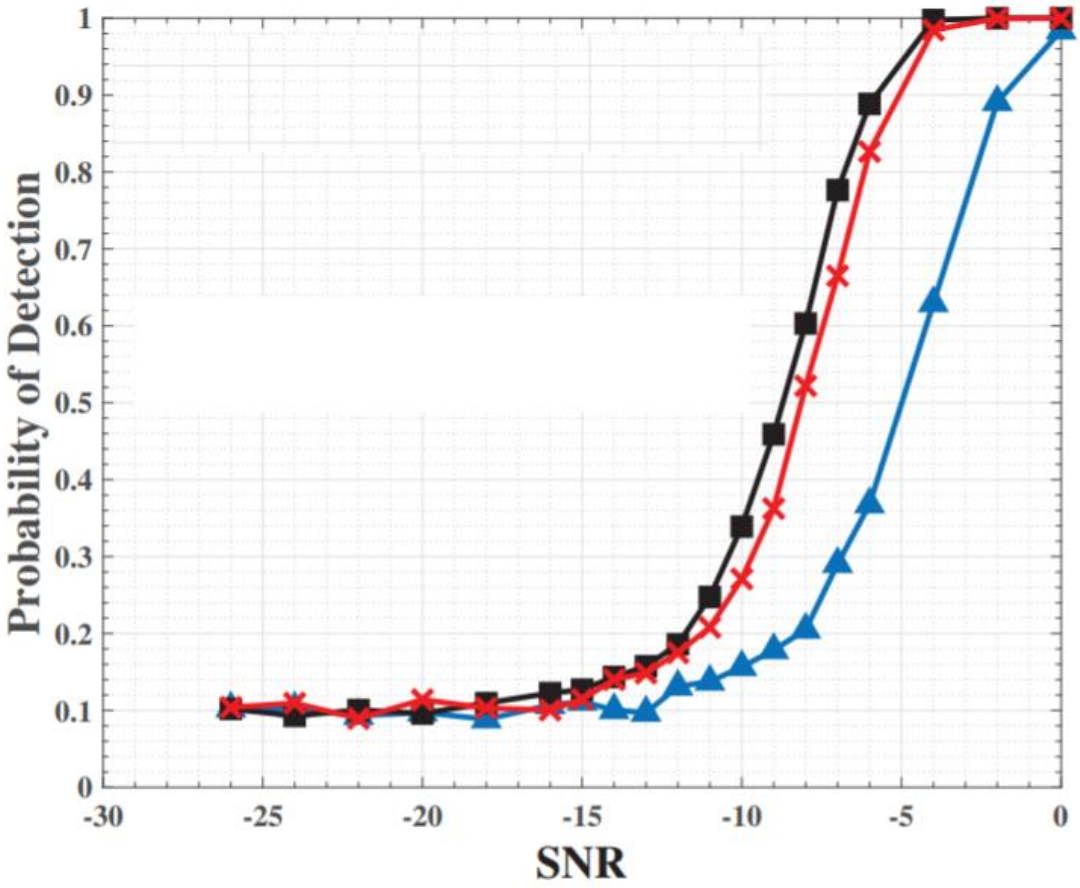

In contrast to the sensor with 1024-point FFT, the efficacy of the recommended 2048-point Spectrum FFT spectrum sensor improves significantly by 3 dB with a chance of 0.8 detection. Although there is a gap of 1 dB from 4096-2048-point FFT sensors at a likelihood of 0.8. In this research, our 2048-point FFT spectrum sensor has been implemented, which provides a probability of detection of 0.9 in SNR at -5 dB, as shown in Fig. 5. Though applying an FFT-based spectrum sensor of 1024-point decreases the area use the sensors' performance in the low SNR zone would deteriorate. Furthermore for 2048–4096 FFT, the performance of the spectrum sensor is weak compared to 1024–2048 FFT. This makes the 2048-point FFT sensor optimum for a stronger hardware performance production.

5. CONCLUSION

The CFD-based spectrum sensor architecture was built in these works to detect signal reliably in low SNR areas. With a modern 2048-point FFT unit architecture that consumes full region in our sensor, the memory-free architecture of the spectre sensor is built. This paper proposes CFD dependent spectrum sensors that consume fewer hardware and have shorter sensing periods for cognitive radio technologies. The problem of applying complex CFD spectrum sensing algorithms dependent on frequencies was discussed. The proposed architecture implements the memory-free FFT algorithm and allows fast sensing time. Our efficiency analyses are provided for 1024, 2048 and 4096 point FFT sizes, with sufficient likelihood of detection of 0.9 at -5 dB of SNR in the proposed architecture.

Reference

[1]. Salahdine F, Kaabouch N, El Ghazi H. A Bayesian recovery technique with Toeplitz matrix for compressive spectrum sensing in cognitive radio networks. International Journal of Communication Systems. 2017 Oct; 30(15):e3314.

[2]. U.Jeyamalar, N.Mangaiyarkarasi, T.Jayasankar, ”FPGA Implementation Time Efficient High Performance VLSI Adders,”National Conference on Digital Processing and Communication in Anna University of Technology Tiruchirappalli on April 2011.

[3]. Sardar M, Karthikeyan KV. Study on sensing techniques for cognitive radio network: A survey. In2016 International Conference on Circuit, Power and Computing Technologies (ICCPCT) 2016 Mar 18 (pp. 1-7). IEEE.

[4]. Amrutha V, Karthikeyan KV. Spectrum sensing methodologies in cognitive radio networks: A survey. In2017 International Conference on Innovations in Electrical, Electronics, Instrumentation and Media Technology (ICEEIMT) 2017 Feb 3 (pp. 306-310). IEEE.

[5]. Anyim IG, Chiverton J, Filip M, Tawfik A. The implementation of wideband cyclostationary feature detector with receiver constraints. In2017 European Conference on Networks and Communications (EuCNC) 2017 Jun 12 (pp. 1-5). IEEE.

[6]. Anyim IG, Chiverton J, Filip M, Tawfik A. The optimization of wideband cyclostationary feature detector with receiver constraints.

[7]. Nandini KS, Hariprasad SA. A Survey of Spectrum Sensing Mechanisms in Wireless Cognitive Radio Networks. In2017 14th IEEE India Council International Conference (INDICON) 2017 Dec 15 (pp. 1-6). IEEE.

[8]. Chaurasiya RB, Shrestha R. Hardware-Efficient and Fast Sensing-Time Maximum-Minimum-Eigenvalue-Based Spectrum Sensor for Cognitive Radio Network. IEEE Transactions on Circuits and Systems I: Regular Papers. 2019 Jun 26;66(11):4448-61.

[9]. Mansour A, Tayel AF, Khames A, Azab M, Rabia SI, Shehata N. Towards software defined antenna for cognitive radio networks through appropriate selection of RF-switch using reconfigurable antenna array. AEU-International Journal of Electronics and Communications. 2019 Apr 1;102:25-34.